

Title	DOUBLE SYMBOL ERROR RATE AND BLOCK ERROR RATE OF MDPSK
Author(s)	Adachi, F.; Matsumoto, T.
Citation	Electronics Letters, 27(17): 1571-1573
Issue Date	1991-08-15
Type	Journal Article
Text version	publisher
URL	http://hdl.handle.net/10119/4804
Rights	<p>Copyright (c)1991 IEEE. Reprinted from Electronics Letters, 27(17), 1991, 1571-1573.</p> <p>This material is posted here with permission of the IEEE. Such permission of the IEEE does not in any way imply IEEE endorsement of any of JAIST's products or services. Internal or personal use of this material is permitted. However, permission to reprint/republish this material for advertising or promotional purposes or for creating new collective works for resale or redistribution must be obtained from the IEEE by writing to pubs-permissions@ieee.org. By choosing to view this document, you agree to all provisions of the copyright laws protecting it.</p>
Description	



current density of 1.81 kA cm^{-2} for broad area lasers ($50 \mu\text{m} \times 300 \mu\text{m}$) was obtained at 628 nm.

H. MURATA
Y. TERUI
M. SAITOH
Y. SATOH
R. TERASAKI

2nd July 1991

Electronic Material Department
Research Center
Denki Kagaku Kogyo Co., Ltd.
3-5-1 Asahimachi
Machidashi, Tokyo 194, Japan

References

- ISHIKAWA, M., OKUDA, H., ITAYA, K., SHIOZAWA, H., and UEMATSU, Y.: 'Long-term reliability tests for InGaAlP visible laser diodes', *Jpn. J. Appl. Phys.*, 1989, **28**, pp. 1615-1621
- KIKUCHI, A., KANEKO, Y., NOMURA, I., and KISHINO, K.: 'Room temperature continuous wave operation of GaInP/AlInP visible-light laser with GaInP/AlInP superlattice confinement layer grown by gas source molecular beam epitaxy', *Electron. Lett.*, 1990, **26**, pp. 1668-1669
- ITAYA, K., ISHIKAWA, M., and UEMATSU, Y.: '636 nm room temperature CW operation by heterobarrier blocking structure InGaAlP laser diodes', *Electron. Lett.*, 1990, **26**, pp. 839-840
- KOBAYASHI, K., UENO, Y., HOTTA, H., GOMYO, A., TADA, K., HARA, K., and YUASA, T.: '632.7 nm CW operation (20°C) of AlGaInP visible laser diodes fabricated on (001) 6° off toward (110) GaAs substrate', *Jpn. J. Appl. Phys.*, 1990, **29**, pp. L1669-L1671
- HAMADA, H., SHONO, M., HONDA, S., HIROYAMA, R., MATSUKAWA, K., YODOSHI, K., and YAMAGUCHI, T.: 'High-power operation of 630 nm-band transverse-mode stabilised AlGaInP laser diodes with current-blocking region near facets', *Electron. Lett.*, 1991, **27**, pp. 661-662
- HINO, I., GOMYO, A., KAWATA, S., KOBAYASHI, K., and SUZUKI, T.: 'Magnesium doping of AlGaInP grown by metalorganic chemical vapor deposition', *Inst. Phys. Conf. Ser.*, 1986, **79**, pp. 151-156
- OHBA, Y., NISHIKAWA, Y., NOZAKI, C., SUGAWARA, H., and NAKANISI, T.: 'A study of p-type doping for AlGaInP grown by low-pressure MOCVD', *J. Cryst. Growth*, 1988, **93**, pp. 613-617
- NELSON, A. W., and WESTBROOK, L. D.: 'A study of p-type dopants for InP grown by adduct MOVPE', *J. Cryst. Growth*, 1984, **68**, (1), pp. 102-110
- VEUHOF, E., BAUMEISTER, H., TREICHLER, R., and BRANDT, O.: 'Mg diffusion during metalorganic vapor phase epitaxy of InP', *Appl. Phys. Lett.*, 1989, **55**, pp. 1017-1019
- DEPPE, D. G., NAM, D. W., HOLONYAK, N., JUN., HSIEH, K. C., and BAKER, J. E.: 'Impurity-induced layer disordering of high gap InAlGaP heterostructures', *Appl. Phys. Lett.*, 1988, **52**, pp. 1413-1415

DOUBLE SYMBOL ERROR RATE AND BLOCK ERROR RATE OF MDPSK

Indexing terms: Errors, Digital communication systems

The double symbol error rate (DSER) is calculated for an M -ary DPSK (MDPSK) system to show that double symbol errors are less likely to be produced when $M \geq 4$ than for the binary case ($M = 2$) and that MDPSK with $M \geq 4$ provides similar conditional SER (defined as the SER when the previous symbol decision was in error) when compared at the same SER value. The block error rate (BKER) is also shown to be well approximated by that determined assuming independent symbol error when $M \geq 4$.

Introduction: Error control, such as forward error correction (FEC) and automatic repeat request (ARQ), is often used to improve bit error rate (BER) performance. In M -ary differential phase shift keying (MDPSK) systems, symbol errors tend to be produced in pairs due to differential detection. When the phase of the signal plus additive noise at decision time $t = nT$ is represented by θ_n , the n th symbol is determined from $\Delta\theta_n = \theta_n - \theta_{n-1}$ and the $(n-1)$ th symbol from $\Delta\theta_{n-1} = \theta_{n-1} - \theta_{n-2}$.

Therefore, if noise forces a large phase deviation in θ_{n-1} , two consecutive symbol errors (double symbol error) are likely to be produced. Statistics of symbol error patterns affect the FEC performance. In this Letter, the double symbol error rate (DSER) of an M -ary DPSK (MDPSK) system is calculated. When ARQ is used (no FEC is incorporated), retransmission is requested if the received data block contains at least one single error. This Letter also calculates the block error rate (BKER) taking into account the effect of double symbol error.

Calculation of DSER: Oberst and Shilling¹ calculated the DSER for 2DPSK (or BDPSK). Goldman² extended the analysis to MDPSK (however, the calculated results were shown only for $M = 2$ and 4). We present a simple, approximate DSER calculation method and calculate the conditional SER which is defined as the SER when the previous symbol decision was in error.

The phase of detector input signal is fluctuated by additive noise. Let ϕ be the phase error of θ_{n-1} from the ideal phase point $\Theta = m\pi/M$, $m = 0, 1, \dots, M-1$, at decision time $t = (n-1)T$. The n th symbol and $(n-1)$ th symbol are correctly detected if the phase errors of θ_n and θ_{n-2} lie between $\phi + \pi/M$ and $\phi - \pi/M$. Assuming that noise samples are independent Gaussian variables, SERs of the n th and $(n-1)$ th symbols, when the phase error of θ_{n-1} is ϕ , can be given by

$$\begin{aligned} p(E_n | \phi) &= p(E_{n-1} | \phi) \\ &= \frac{1}{2} \operatorname{erfc} \left[\sqrt{\gamma} \sin \left(\frac{\pi}{M} + \phi \right) \right] \\ &\quad + \frac{1}{2} \operatorname{erfc} \left[\sqrt{\gamma} \sin \left(\frac{\pi}{M} - \phi \right) \right] \\ &\quad - \frac{1}{4} \operatorname{erfc} \left[\sqrt{\gamma} \sin \left(\frac{\pi}{M} + \phi \right) \right] \\ &\quad \times \operatorname{erfc} \left[\sqrt{\gamma} \sin \left(\frac{\pi}{M} - \phi \right) \right] \end{aligned} \quad (1)$$

where γ is the signal-to-noise ratio. Eqn. 1 is an exact expression for 4DPSK (or QDPSK). For MDPSK with $M \geq 8$, however it is an upper bound. Because the third term in the right hand side of eqn. 1 is negligible for large values of γ , eqn. 1 gives a good approximation. SER $P(E_n)$ is obtained by averaging $p(E_n | \phi)$ with the probability density function $p(\phi)$ of ϕ .²

$$\begin{aligned} p(\phi) &= \frac{1}{2\pi} e^{-\gamma} + \frac{1}{2} \sqrt{\frac{\gamma}{\pi}} e^{-\gamma \sin^2 \phi} \\ &\quad \times \cos \phi \{ 1 + \operatorname{erf} [\sqrt{\gamma} \cos \phi] \} \end{aligned} \quad (2)$$

Because error events E_n and E_{n-1} are independent, DSER can be calculated from

$$P(E_n, E_{n-1}) = \int_{-\pi}^{\pi} p(E_n | \phi) p(E_{n-1} | \phi) p(\phi) d\phi \quad (3)$$

Finally, conditional SER $P(E_n | E_{n-1})$ can be obtained from $P(E_n, E_{n-1})/P(E_{n-1})$.

Fig. 1 shows the calculated results of the conditional SER as a function of signal energy per bit-to-noise power spectrum density ratio ($E_b/N_0 = \gamma/\log_2 M$). For comparison, SER is also shown (it was found that SER performance when $M \geq 8$ is almost identical with the exact one calculated from Reference 4). It can be seen that the conditional SER of BDPSK decreases very slowly and is larger than that of QDPSK when $E_b/N_0 > 4$ dB. The conditional SERs at various values of SER were obtained from Fig. 1 and compared in Fig. 2. At an SER of 10^{-3} , the conditional SERs are 1.8×10^{-1} for $M = 2$, 5.0×10^{-2} for $M = 4$, 3.6×10^{-2} for $M = 8$, and 3.4×10^{-2} for $M = 16$. It can be seen that when compared at the same SER value, the conditional SER is largest for BDPSK and those for MDPSK with $M \geq 4$ are similar. The reason why

the conditional SER of BDPSK is larger than those of the other schemes can be qualitatively explained. Because of the larger decision phase margin ($\pm \pi/2$) of BDPSK, the $(n-1)$ th

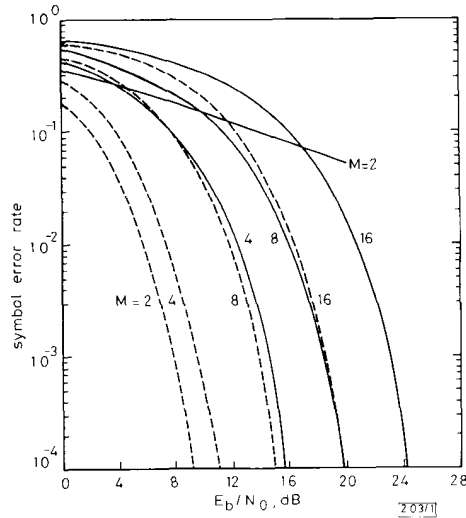


Fig. 1 Conditional SER MDPSK
 — conditional SER
 - - - SER

symbol is erroneously detected when a large phase error of θ_{n-1} occurs. However, it is rare for the phase error of θ_n to have the same sign and be able to cancel the effect of the previous phase error. This produces double symbol error. As M increases, however, the decision phase margin decreases and smaller phase error of θ_{n-1} causes an error in the $(n-1)$ th symbol. Therefore, it is more likely for the phase error of θ_n to cancel the effect of phase error of θ_{n-1} , so that double errors tend to be reduced.

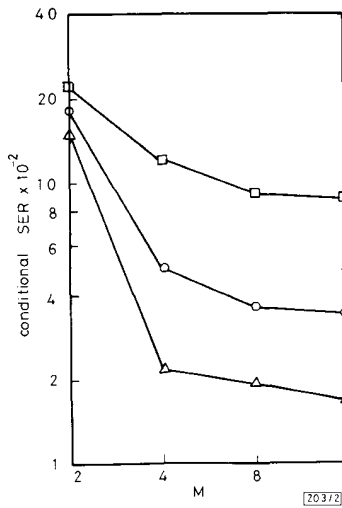


Fig. 2 Comparison of conditional SERs at various SERs
 □ SER = 10^{-2}
 ○ SER = 10^{-3}
 △ SER = 10^{-4}

Block error rate: Here, BKER is defined as the probability of the data block containing at least one single error. An N -symbol block is assumed. Because nonadjacent symbol deci-

sions are independent, BKER can be calculated from

$$BKER = 1 - P(C_0) \prod_{j=1}^{N-1} P(C_j | C_{j-1}) \quad (4)$$

where C_j is the event of correction decision for the j th symbol. $P(C_j | C_{j-1})$ is identical for any j , and eqn. 4 can be rewritten as

$$BKER = 1 - P(C_0) \cdot P^{N-1}(C_1 | C_0) \quad (5)$$

where $P(C_0) = 1 - P(E_0)$, $P(C_1 | C_0) = P(C_0, C_1) / P(C_0)$. Note that $P(E_0) = P(E_1)$ and $P(C_0, C_1) = 1 - 2P(E_1) + P(E_0, E_1)$. Fig. 3 shows the calculated BKER performance for $N = 64$.

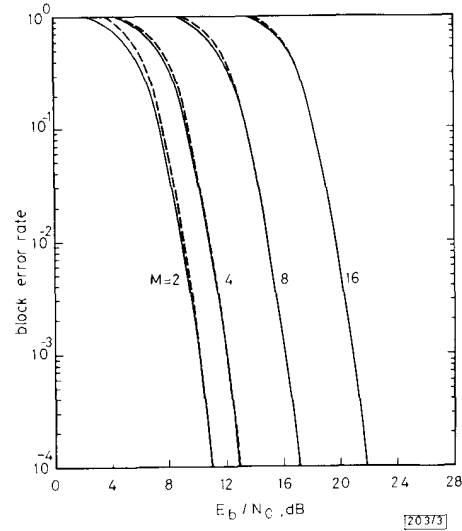


Fig. 3 BKER performance
 — eqn. 5
 - - - independent error
 Block length $N = 64$
 MDPSK

Eqn. 5 can be approximated as

$$BKER \approx N \cdot P(E_0) [1 - P(E_1 | E_0)] \quad (6)$$

for a high E_b/N_0 . If symbol errors are independent, then $BKER = 1 - \{1 - P(E_0)\}^N \approx N \cdot P(E_0)$. Hence, the BKER with differential detection is smaller by a factor of $1 - P(E_1 | E_0)$ than that experienced with independent symbol error. It is found from Fig. 1 that the BKER of BDPSK becomes 72% of that determined assuming independent symbol error when $E_b/N_0 = 8$ dB. For $M \geq 4$, however, because $1 - P(E_1 | E_0)$ is very small, the effect of double symbol error is negligible. This is confirmed by Fig. 3 in which BKER performance is plotted assuming independent symbol error.

Conclusion: The conditional SER of MDPSK with $M \geq 4$ is much smaller than that of BDPSK when compared at the same SER value. The effect of double symbol errors on BKER is negligible and therefore BKER is well approximated by that determined assuming independent symbol error when $M \geq 4$.

F. ADACHI
 T. MATSUMOTO

5th July 1991

NTT Radio Communication Systems Laboratories
 1-2356 Take
 Yokosuka-shi, Kanagawa-ken 238, Japan

References

- OBERST, J. F., and SCHILLING, D. L.: 'Double error probability in differential PSK', *Proc. IEEE*, June 1968, pp. 1099-1100

- 2 GOLDMAN, J.: 'Multiple error performance of PSK systems with cochannel interference and noise', *IEEE Trans.*, August 1971, **COM-19**, pp. 420-430
- 3 BENNETT, W. R.: 'Method of solving noise problems', *Proc. IRE*, May 1956, **44**, pp. 609-638
- 4 PAWULA, R. F.: 'Asymptotics and error bounds for M-ary DPSK', *IEEE Trans.*, January 1984, **COM-32**, pp. 93-94

NOVEL LEAKY-WAVE ANTENNA FOR MILLIMETRE WAVES BASED ON V-GROOVE GUIDE

Indexing terms: Antennas, Waveguides

A novel type of leaky-wave antenna for millimetre waves based on the V-groove guide is described. A complete transverse equivalent network is presented for analysis and design of this new leaky-wave antenna. Numerical results for the performance characteristics of the antenna are given.

Introduction: The groove guide is potentially attractive as a low-loss waveguide in millimetre wave and submillimetre wave bands. Recently this kind of waveguiding structure has attracted increasing attention because of its advantages such as low-loss nature, ease of fabrication, large structural dimensions and higher power handling capacity. A leaky-wave antenna constructed from the groove guide was described and investigated by Oliner and Lampariello.¹⁻³ This leaky groove guide antenna overcomes two problems that leaky-wave antennas for millimetre wave ranges often face: lower wavelengths and higher metal loss. The V-groove guide is an alternative to the rectangular-groove guide. The new structure exhibits lower attenuation and more effective rejection of higher order modes. Based on the V-groove guide, we present a new type of leaky-wave antenna. An accurate analysis, based on a transverse equivalent network, is presented for the properties of this leaky structure that takes into account the mode conversion from the bound mode to the leaky mode. Using this analysis, numerical design values can be readily obtained. The antenna structure is therefore able to be easily understood and systematically designed.

Analysis: The cross-section of the new leaky-wave antenna is shown in Fig. 1. As in References 1-3, it is the added continuous strip of width δ that introduces asymmetry into the basic V-groove guide and creates the leakage. The strip therefore gives rise to an additional transverse mode and couples that mode to the original transverse mode which by itself would be purely bound.

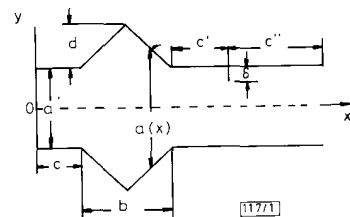


Fig. 1 Cross-section of new leaky-wave antenna based on V-groove guide

The transverse equivalent network for the cross-section of the structure shown in Fig. 1 is given in Fig. 2. This network is based on these two transverse modes, which propagate in the x direction and are coupled by the narrow asymmetrical strip. These coupled transverse modes then combine to produce a net TE longitudinal mode (in the y direction) with a complex propagation constant $\beta - j\alpha$. In the network, the $i = 1$ transmission lines represent the original mode with a half-sinewave variation in the y direction in Fig. 1, and the $i = 0$ transmission lines represent the new mode which has no variation with y . In the central region, the tapered lines represent the V

groove, which can be analysed by a numerical integration technique. The detailed formulation of the analysis method for the tapered lines can be found in a recent paper.⁵

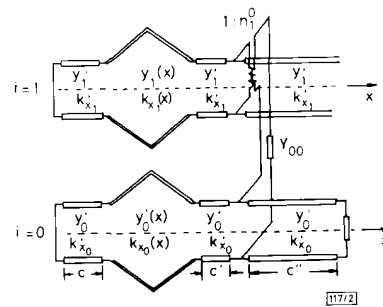


Fig. 2 Complete transverse equivalent network for structure whose cross-section is shown in Fig. 1

The expressions for the various constituents of this network can be found in References 3 and 6. The final expression for β and α can be derived by the application of the transverse resonance condition.

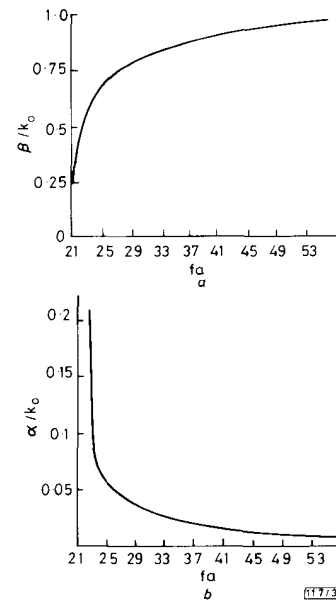


Fig. 3 Variation of normalised phase constant β/k_0 and leakage constant α/k_0 with normalised frequency in form fa

f is in GHz
 a is in cm
 (a) β/k_0 against fa
 (b) α/k_0 against fa
 $a'/a = 0.68$
 $b/a = 0.4$
 $c/a = 1.28$
 $c'/a = 0.20$
 $c''/a = 1.50$
 $\delta/a = 0.25$

Numerical results: We have obtained numerical values in graphical form of the variation of β and α with each of these dimensional parameters, so that design optimisation can proceed in a systematic fashion. However, we present here, in Figs. 3a and b, respectively, only the curves of β/k_0 and α/k_0 as a function of fa (where f is the frequency in GHz and a is the width of the central region in cm). It can be seen that the performance of the new V-groove guide leaky-wave antenna is very similar to that of the leaky rectangular-groove guide antenna. Because the cutoff wavelength of the V-groove guide is bigger than that of the rectangular-groove guide with the